

Analytical, Computational Fluid Dynamics and Flight Dynamics of Coandă MAV

H Djojodihardjo¹ and RI Ahmed²

¹The Institute for the Advancement of Aerospace Science and Technology, Jl. Uranus V-17, Jakarta 15419, Indonesia; harijono.djojodihardjo@yahoo.com; engriyadh64@gmail.com

²Graduate Student, Aerospace Engineering Department, Universiti Putra Malaysia, 43400 UPM Serdang, Selangor, Malaysia

Abstract. The paper establishes the basic working relationships among various relevant variables and parameters governing the aerodynamics forces and performance measures of Coandă MAV in hover and translatory motion. With such motivation, capitalizing on the basic fundamental principles, the Fluid Dynamics and Flight Mechanics of semi-spherical Coandă MAV configurations are revisited and analyzed as a baseline. To gain better understanding on the principle of Coandă MAV lift generation, a mathematical model for a spherical Coandă MAV is developed and analyzed from first physical principles. To gain further insight into the prevailing flow field around a Coandă MAV, as well as to verify the theoretical prediction presented in the work, a computational fluid dynamic CFD simulation for a Coandă MAV generic model are elaborated using commercial software FLUENT®. In addition, the equation of motion for translatory motion of Coandă MAV is elaborated. The mathematical model and derived performance measures are shown to be capable in describing the physical phenomena of the flow field of the semi-spherical Coandă MAV. The relationships between the relevant parameters of the mathematical model of the Coandă MAV to the forces acting on it are elaborated subsequently.

1. Introduction

Coandă effect and Coandă jet have found many applications in engineering, among others in aircraft and vehicle technology [1-5], as well as wind-turbines [6-9]. In particular, Coandă MAV share in active developments, and various configurations have been proposed and developed. For the purpose of designing a Coandă MAV which could meet the desired mission and design requirements, it is mandatory to establish the basic working relationships among various relevant variables and parameters governing the aerodynamics forces. To assist the analysis, design and developments of Coandă MAV's, several tools can be resorted to. The first is the analytical tool, which capitalizes on the basic fundamental principles. The second is the utilization of Computational Fluid Dynamics, (CFD) which has the advantage of providing visualization for significant insight and identification to the problem at hand, which then can be utilized in enhancing the analysis and identifying specific details. Experimental tools can benefit from the insight gained by analysis, CFD computational and visualization studies, in the preliminary study stage by designing specific experiments as well as in the conceptual and prototype design stages. Various CFD studies have also indicated that there are still significant discrepancies between CFD and experimental studies [6], which necessitate the existence of specific baseline configurations for validation purposes. Coandă MAV is expected to be capable of manoeuvring, and the analysis carried out here is associated with hovering and cruising conditions, which should give further insight on, and can be further elaborated into its manoeuvring performance.



In the study of Coandă MAV, it is desired that the Coandă propulsion system will be able to provide both an efficient cruise phase as well as hover capability, by using Coandă jet blanket for semi-spherical Coandă MAV, which is deflected downward using a curved surface. Thus lift will be generated, first to hover and later for propulsion as well. Such Coandă jet has been utilized for circulation enhancement [3-9] for fixed wing aircraft and turbine blades in forward flight and movement. The principle of Coandă MAV lift generation as well as the equation of motion for its translatory motion will be derived and elaborated.

The present analysis is carried out on Coandă MAV spherical configuration as a baseline, which utilizes some results from the authors' previous analysis. The equations can be easily modified for other configurations and can be compared to other investigators' results for further assessments. CFD visualization studies will also be utilized to gain further understanding in developing the physical model in the analysis.

Some basic results drawn from the physical and mathematical model has been obtained to describe the physical phenomena of the flow field related to the relevant surfaces influenced by the Coandă effect jet sheets, and rewritten in a more convenient form as necessary to gain better insight on the relationship among the relevant parameters.

2. System of Coordinates

For the derivation of the equation of motion of the Coandă MAV, the system coordinates that are required for setting the equation will be defined. Following the convention in flight dynamics, four main reference frames are identified, namely the inertial coordinate system, the local horizon reference frame, the body reference frame, and the wind reference frame, as required in the analysis, and are depicted in Figure 1a. Without loss of generality, for simplicity and instructiveness, only two-dimensional coordinate systems in the plane of symmetry of the Coandă MAV will be elaborated. These four coordinates are:

- Inertial coordinate system**, which is used for defining and the application of the Newton's law of motion. In two dimensions, this coordinate system is depicted by the O_{ExyZ} .
- The local horizon coordinate system $O_{x_h y_h z_h}$** , which is fixed at the center of mass of the vehicle, and is parallel with the earth Inertial Coordinate system.

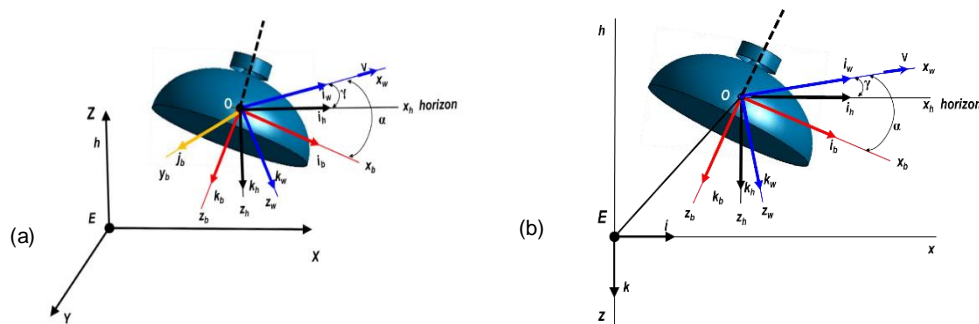


Figure 1. (a) The details of the four coordinate systems for Coandă MAV flight vehicle; (b) Axes systems in the vertical plane perpendicular to the Earth's Surface

- The body coordinate system $O_{x_b y_b z_b}$** , which is fixed to the vehicle, and follows a conveniently chosen axis of the vehicle.
- The wind axes system $O_{x_w y_w z_w}$** , which moves with the vehicle and the x_w axis is coincident with the velocity vector (flight path of the vehicle).

In the figure, the wind axes are oriented to the flight path angle γ relative the local horizon axes and by the angle of attack α relative to the body axes. The two dimensional configuration in the vertical plane perpendicular to the earth surface is shown in Figure 1 (b).

3. Mathematical Model and Fluid Dynamic Analysis for hovering Semi-spherical Coandă MAV as a Baseline Configuration

The mathematical model of Coandă MAV elaborated here follows closely that of Ahmed et al [10-11] and Djojodihardjo and Ahmed [12-13], which was based on first principles and are summarized and reproduced here as a baseline reference for other development. For Coandă MAV with the configuration depicted in Figure 2, an actuator rotor can be visualized to be located at the center of the body. For conceptual development, the dimension of the rotor can be set to be small. Part of the flow being drawn by the actuator can be utilized for lift (like in a helicopter), and part of it will be utilized for establishing radial flow for Coandă jet blanket on the surface of the body. Momentum analysis is carried out in the analysis of Coandă effect related to finding the relevant aerodynamic forces and defining the Coandă MAV performance parameters. The latter is developed for a baseline and simplified semi-spherical Coandă MAV as depicted in Figure 3. In the following, a rigorous analysis is carried out to elaborate how Coandă effect contributes to the generation of lift capability of Coandă MAV.

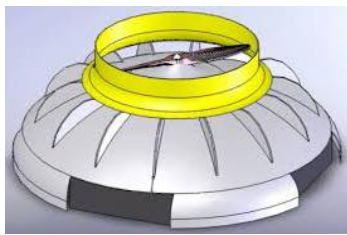


Figure 2. A semi-spherical Coandă MAV indicating the development of Coandă jet over the upper surface of the Coandă MAV.

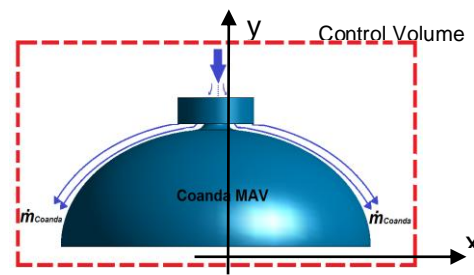


Figure 3. An equivalent Semi-Spherical Coandă MAV for generic analysis.

First, the analysis will address the Coandă effect for lift by applying the fundamental conservation analysis on the control volume CV (red dashed rectangle in Figure 3).

Applying the continuity equation on the control volume, which reduces to the Coandă Blanket as depicted in Figure 3b, there is obtained

$$\rho \cdot V_{j-R} \cdot 2\pi R h = \rho \cdot V_{j-in} \cdot 2\pi R_i h_i = \rho \cdot V_{j-out} \cdot 2\pi R_o h_o \quad (1)$$

and

$$V_{j-R} = \frac{R_i h_i}{R h_R} V_{j-in} = \frac{\dot{m}}{2\pi \rho R h_R} \quad (2)$$

$$V_{j-out} = \frac{R_i h_i}{R_o h_o} V_{j-in} = \frac{\dot{m}}{2\pi \rho R_o h_o}$$

where V_{j-R} is the jet flow velocity, R is the vehicle body radius, h is the jet slot thickness and \dot{m} is the jet mass flow rate. The momentum equation applied to the control volume in the y (vertical) direction can be differentiated into the contribution due to the Coandă Blanket momentum and the pressure difference on the body due to Coandă Blanket:

$$\left(\begin{array}{c} \text{Total Lift force} \\ \text{due to Coandă Blanket} \end{array} \right) = \left(\begin{array}{c} \text{Vertical component of momentum} \\ \text{balance due to Coandă Blanket} \end{array} \right) + \left(\begin{array}{c} \text{Pressure difference on the body} \\ \text{of MAV subject to Coandă Blanket} \end{array} \right) \quad (3)$$

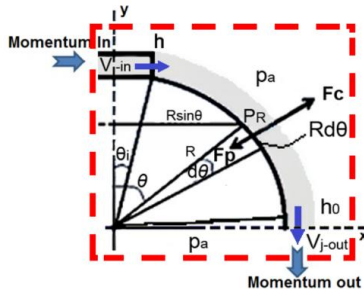


Figure 4. Schematic of Coandă jet (Blanket) for a Spherical (doughnut shaped) MAV.

The contribution of lift from the momentum flux through the control volume CV in the y (vertical) direction is given by:

$$\left(\begin{matrix} \text{Force in the} \\ \text{y-direction} \end{matrix} \right) = \left(\begin{matrix} \text{Momentum Out} \\ \text{in the y-direction} \end{matrix} \right) - \left(\begin{matrix} \text{Momentum In} \\ \text{in the y-direction} \end{matrix} \right) \quad (4)$$

Since the Momentum in the radial direction does not contribute to lift, then the momentum equation in the y-direction for the control volume CV depicted in Figure4 is:

$$F_{\text{Coanda jet Blanket}} = \dot{m} V_{j-out} = 2\pi R_i h_i \rho \cdot V_{j-in} \cdot V_{j-out} \quad (5)$$

The contribution of lift from the pressure difference between the upper part (curved MAV body covered by Coandă Blanket) and the lower part of the MAV body can be found by considering various fundamental physical approach. The detail of the elaboration can be found in Ahmed and Djojodihardjo [10-11] and yields:

$$F_{\text{Induced pressure difference}} = F_{\text{lower-surface}} - F_{\text{upper-surface}} = \pi (R_o^2 - R_i^2) p_a - \int_{\theta_i}^{\theta_o} \left(p_a - \frac{h}{R} \rho \left(\frac{\dot{m}}{2\pi \rho R h} \right)^2 \right) \pi R^2 \sin 2\theta d\theta \quad (6)$$

where θ_i and θ_o are the turning angles at which the jet flow injected and separated from the Coandă surface respectively, as depicted in Figure4. The jet flow assumed to be uniform outflow separating at the sharp edge of the Coandă MAV curved surface. Then the contribution for lift due to the pressure difference across the surfaces of the MAV body, for the latter approach is given by (as elaborated by Djojodihardjo and Ahmed [12-13]), for the significant value of θ_i :

$$F_{\text{Induced pressure difference}} = \left(\frac{\dot{m}^2}{4\pi \rho h_R R} \right)_{j-R} \quad (7)$$

Hence the total lift due to Coandă jet blanket momentum and Coandă jet blanket induced pressure difference is given by

$$Lift_{\text{Spherical-Coanda jet Blanket+ induced pressure difference}} = 2\pi R_i h_i \rho V_{j-in} \cdot V_{j-out} + \left(\frac{\dot{m}^2}{4\pi \rho R h} \right)_{j-out} = \dot{m} \cdot V_{j-out} + \frac{1}{2} \dot{m} V_{j-out} \quad (8)$$

Hence, due to the presence of the Coandă blanket, the Coandă MAV has additional lift given in (8). It should be noted that a more exact approach requires additional information, i.e. the energy conservation equation, which is then utilized as the fourth equation. This is elaborated subsequently.

Applying the energy conservation equation on the same control volume, which has been redrawn for convenience in Figure5, assuming uniform properties across the sectional areas at the input and output of the Coandă jet blanket and ignoring the entrainment energy exchange between the ambient air and the Coandă jet blanket, the energy equation can be written as:

$$\left(\frac{p}{\rho} \right)_{in} + \frac{1}{2} (V_{j-in}^2) = \left(\frac{p}{\rho} \right)_{out} + \frac{1}{2} (V_{j-out}^2) \quad (9)$$

which is essentially the Bernoulli equation along any streamline between the inlet and the outlet sections. The contribution of the entrainment energy exchange along the Coandă jet blanket can later be incorporated, such as by adopting certain assumptions as a heuristic approach or, applying the complete viscous equation by numerical simulation or CFD approach.

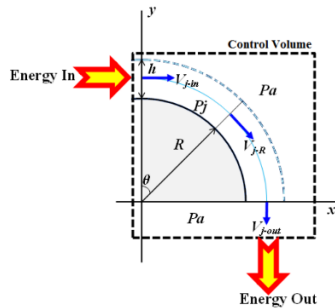


Figure 5. Schematic of the control volume around the MAV for the application of the energy.

The latter should be carried out for more meticulous approach, using the present simplified analytical approach as guidelines. At the same time, the CFD results, by appropriate considerations of the relevant parameters utilized there can be used in developing the heuristic approach as well as for validating and assessing the merit of the analytical approach. Noting that from the outset, the flow is considered to be incompressible, equation (9) reduces to

$$\frac{1}{2}\rho V_{j-in}^2 = \frac{1}{2}\rho V_{j-out}^2 \quad (10)$$

Hence, by the application of the conservation energy principle for incompressible flow, and assuming ambient pressure at the inlet and outlet of the Coandă jet blanket and neglecting the energy exchange between the ambient air and the Coandă jet blanket, the following velocity relationship between the inlet and outlet sections of the Coandă jet blanket is given by

$$V_{j-out} = V_{j-in} \quad (11)$$

This should simplify the solution given in equation (8) and reduce the use of idealization or the number of assumption since fewer unknowns are included in the equations. Combining equations (8) and (9) yields:

$$Lift_{Coanda-jet\ Blanket+ induced\ pressure\ difference} = \frac{3}{2}\dot{m}V_{j-in} \quad (12)$$

The results will be assessed a posteriori by using more structured CFD simulations, although the latter also contain uncertainties and inaccuracies.

Mathematical Model and Flight Dynamic Analysis for Semi-spherical Coandă MAV in Translatory Motion

In the development of the flight dynamics of Coandă MAV in Translatory Motion, without loss of generalities, the equation of motion is developed in the vertical plane perpendicular to the earth motion, rendering two-dimensional planar motion. The hovering state, as depicted in Figure6, will be utilized as a reference.

Balance of forces in the free-body diagram exhibited in Figure6 and the use of the Coandă lift from equation (12) leads to:

$$L_{Hover} \equiv T_{Coandă-MAV} = \frac{3}{2} \dot{m} \cdot V_{j-in} = 3\pi\rho R_i h_i V_{j-in}^2 = W_{Coandă-MAV-Take-off} \quad (13)$$

In the development of the equation of motion during translatory motion, a further simplifying assumptions will be made, which could be refined at later stage to incorporate more realistic ones.

These are:

1. The thrust of the Coandă MAV will not be affected by the attitude of the Coandă MAV configuration during hover. This assumption implies that Coandă jet flow relative to the Coandă MAV does not change during maneuver. More elaborate analytical model should be developed assisted by CFD simulation.
2. During the translatory motion, the thrust of the Coandă MAV is assumed to be:

$$T_{Coand\ddot{a}-MAV} = \frac{3}{2} \dot{m} \cdot V_{j-in} \Big|_{hover-equivalent} = 3\pi\rho R_i h_i V_{j-in}^2 \Big|_{hover-equivalent} \quad (14)$$

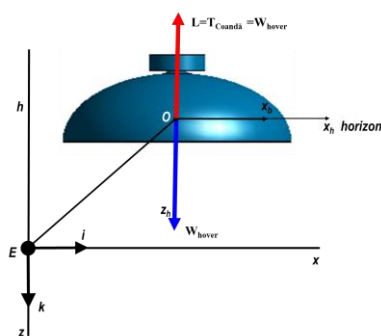


Figure 6. Coordinate systems for Coandă MAV in hover, in two-dimensional configuration (at the vertical plane of symmetry and motion)

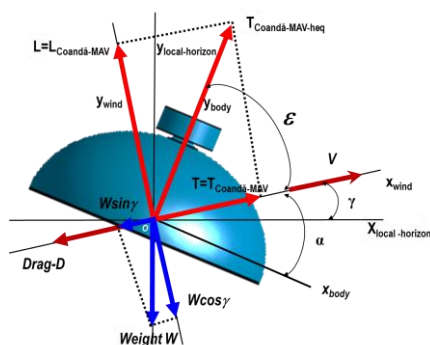


Figure 7. Schematic of Coandă MAV in two-dimensional translatory motion in the vertical plane (at the vertical plane of symmetry and motion)

The equation of motion of the Coandă MAV in translational motion in the two-dimensional vertical plane can be written by referring to Figure 7 using the basic flight dynamic equation for flight vehicle:

Kinematic:

$$\dot{x} = V \cos \gamma \quad \left[LT^{-1} \right] \quad (15)$$

$$\dot{h} \equiv \dot{y} = V \sin \gamma \quad \left[LT^{-1} \right] \quad (16)$$

$$\varepsilon = \tan^{-1} \frac{\ddot{y}_{wind}}{\dot{V}} = \tan^{-1} \frac{g(L - W \cos \gamma)}{W \dot{V}} \quad [-] \quad (17)$$

$$\dot{\mathcal{E}} = \tan^{-1} \frac{\ddot{y}_{wind}}{V} = \tan^{-1} \frac{g(L - W \cos \gamma)}{WV} \quad [T^{-1}] \quad (18)$$

Coandă MAV Fluid Dynamics:

$$T_{Coand\ddot{a}-MAV-heg} \equiv T_{Coand\ddot{a}-MAV-hover-equivalent} = \frac{3}{2} \dot{m} \cdot V_{j-in} = 3\pi\rho R_i h_i V_{j-in}^2 \quad [MLT^{-2}] \quad (19)$$

Coandă MAV Flight Dynamics:

$$\dot{V} = (g / W) (T_{Coandă\ MAV-heq} \cos \varepsilon - D - W \sin \gamma) \quad [LT^{-2}] \quad (20)$$

$$\ddot{y} = (g / W) (T_{Coandă\ MAV-heq} \sin(\varepsilon + \gamma) - W - D \sin \gamma) \quad [LT^{-2}] \quad (21)$$

Weight-Fuel Consumption:

$$\dot{W} = -CT \quad [MT^{-1}] \quad (22)$$

It should be noted, that the above relationships are derived for balance of forces and Newton's equation for semi-spherical Coandă MAV treated as a point mass moving in a plane perpendicular to the planar Earth.

5. Performance Measure

5.1 Performance Measure during Hover

The feasibility of using Coandă techniques to enhance aerodynamic performance of Coandă MAV can be assessed using some non-dimensional quantities of performance measure. The most logical measure that has commonly been utilized is the Coandă jet momentum coefficient, C_μ (Mamou and Khalid [14], 2007; Djojodihardjo [9]),, which are defined as:

$$C_\mu = \frac{\dot{m} V_{Coandă-jet}}{\frac{1}{2} \rho_j V_\infty^2 A_{ref}} \quad (23)$$

While (23) may be appropriate for any Coandă activated vehicle during hover and lift-off, one can define other performance measures to evaluate the aerodynamic performance of the spherical Coandă MAV considered here, based on the rate of the energy of the Coandă jet ejected by Coandă MAV at its ideal inlet velocity V_{j-in} at the Coandă jet injection (inlet) or V_{j-out} at its peripheral outlet compared to the rate of momentum influx of the Coandă jet times its inlet velocity V_{j-in} (non-dimensional):

Further realistic assumption can be drawn from CFD visualization, which also added further insight to the problem. Similar performance measures can be defined for Cylindrically Shaped Coandă MAV.

Taking note that Mirkov and Rasuo [15-16] considered the inlet velocity to thrust ratio for a given inlet size could be the most important output value resulting either from experiment on UAV's or by numerical simulation, another performance measure could be defined to be the lift to inlet velocity, which is a dimensional quantity. Substituting equation (13) for the lift, it gives;

$$PM1_{Spherical\ Coandă-MAV} = \frac{\text{Lift produced by Coandă MAV} \cdot V_{j-out} \text{ at its peripheral outlet}}{\text{the rate of momentum influx of the Coandă jet times its inlet velocity } V_{j-in}} \quad (24)$$

$$= \frac{Lift \cdot V_{j-out}}{\dot{m} V_{j-in}^2} = \frac{\frac{3}{2} \dot{m} V_{j-in}^2}{\dot{m} V_{j-in}^2}$$

$$PM2_{Spherical\ Coandă-MAV} = \frac{Lift_{Coanda-jet\ Blanket+induced\ pressure\ difference}}{Coandă\ jet\ inlet\ Velocity} = \frac{\dot{m} \cdot V_{j-in} + \frac{1}{2} \dot{m} V_{j-in}}{V_{j-in}} = \frac{3}{2} \dot{m} \quad (25)$$

A third performance measure, which is also a dimensional quantity, may be defined based on the Coandă jet rate of momentum influx per unit Coandă jet kinetic energy input [10-11]:

$$PM3_{Spherical\ Coandă-MAV} = \frac{Lift_{Coanda-jet\ Blanket+induced\ pressure\ difference}}{Jet\ Inlet\ velocity^2} = \frac{3}{2} \frac{\dot{m}}{V_{j-in}} \quad (26)$$

5.2 Performance Measure for Translation

Performance measures during translation that are elaborated are:

a. For level flight:

$$\begin{aligned}
 PM_{Coand\ddot{a}-MAV}^{LevelFlight} &= \frac{\text{Power required to overcome Drag}}{\text{Power Input by Coand\ddot{a} - jet - action}} \\
 &= \frac{\text{Drag} * \text{Velocity}}{\text{Coand\ddot{a} Jet Momentum Gain} * \text{Coand\ddot{a} Jet Velocity In}} \\
 &= \frac{D \cdot V \cos \gamma^2}{\dot{m} V_{j-in}^2}
 \end{aligned} \tag{27}$$

For purely level flight, as depicted in Figure 8, $\gamma=0$, and Equation (28) reduces to:

$$PM_{Coand\ddot{a}-MAV}^{LevelFlight} \approx \frac{1}{4} C_{D \rightarrow x} \frac{\pi \rho R_o^2 \sin \alpha}{\dot{m} h_i} \frac{V^3}{V_{j-in}^2} \tag{28}$$

The Performance Measure $PM_{Coand\ddot{a}-MAV}^{LevelFlight}$ can be expressed as a function of C_D , \dot{m} , R_o , h_i , α , V , V_{j-in}

b. For climbing:

$$\begin{aligned}
 PM_{Coand\ddot{a}-MAV}^{Climbing} &= \frac{\text{Power required to Climbing}}{\text{Power Input by Coand\ddot{a} - jet - action}} \\
 &= \frac{\mathbf{T}_{Coand\ddot{a}-MAV-heq} \cdot \dot{\mathbf{y}} - \mathbf{D} \cdot \dot{\mathbf{y}} - \mathbf{W} \cdot \dot{\mathbf{y}}}{\text{Coand\ddot{a} Jet Momentum Gain} * \text{Coand\ddot{a} Jet Velocity In}} \\
 &= \frac{3 \cos(\alpha - \gamma) V \sin \gamma}{2 V_{j-in}} - \frac{(D \sin \gamma + W) V \sin \gamma}{\dot{m} V_{j-in}^2}
 \end{aligned} \tag{29}$$

For purely climbing flight, $\gamma=\pi/2$, and Equation (29) reduces to

$$PM_{Coand\ddot{a}-MAV}^{Climbing} = \frac{\frac{3}{2} \dot{m} \cdot V_{j-in} V - \left(\frac{1}{2} \rho C_{D \rightarrow y} \pi R_o^2 V^2 + W \right) V}{\dot{m} V_{j-in}^2} \tag{30}$$

The Performance Measure $PM_{Coand\ddot{a}-MAV}^{Climbing}$ as function of C_D , R_o , \dot{m} , V , V_{j-in}

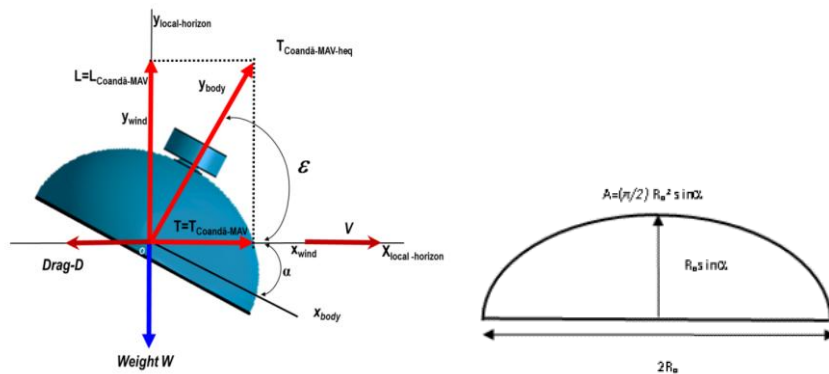


Figure 8. Schematic of Coandă MAV in two-dimensional cruising motion in the vertical plane of symmetry and motion. Inset: Cross sectional area perpendicular to direction of motion.

These are the basic relationships that can further be modified and elaborated for other flight conditions.

6. Some Results and Examples

To assess the merit and plausibility of the theoretical analysis using first principles carried out here, a comparison of the theoretical prediction for the performance measures PM1, PM2 and PM3 given by (25) - (26) are compared with CFD simulation carried out using ANSYS FLUENT® for Spherically Shaped Coandă MAV. The results are depicted in Figs. 9 and 10. The simulation was performed using steady RANS with two equations $k-\omega$ Shear Stress Transport (SST) turbulence model. Simple pressure-velocity coupling scheme with the least squares cell base as discretization gradient was applied in the solution method together with second order upwind for the momentum equation and the turbulent kinetic energy.

The performance $PM2$ as depicted in Figure10 shows the influence of the ratio of the jet slot thickness h to the reference radius R_o . The influence of the jet inlet velocity on the air vehicle performance “lift” may also be of interest from designer’s point of view, which enables them to befittingly select the right propulsion system for such MAV. The jet inlet velocity influence on the performance of the Spherical Coandă MAV at constant jet thickness ($h=50\text{mm}$) is depicted in Figure11. For comparative and validation purposes, Figs. 12 (a) and (b) are produced to assess the present theoretical prediction with CFD simulation results for the case considered by Schroyen and van Tooren [15] for cylindrical Coandă MAV, for $h/R=0.075$ at two different jet inlet velocities.

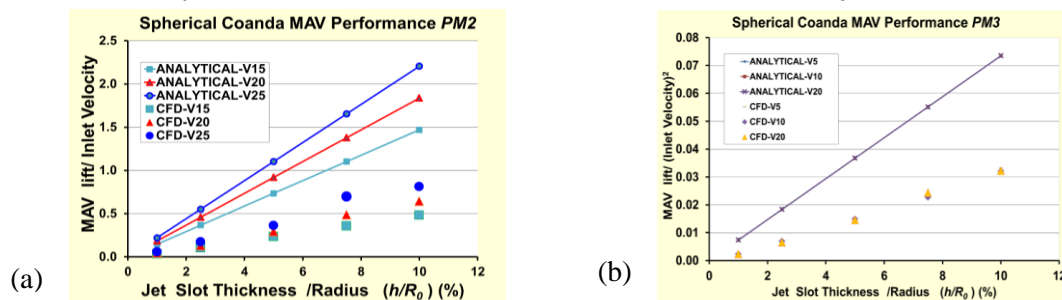


Figure 9. Qualitative comparison of analytical (non-viscous) and CFD (viscous) computed Performance Measure for spherical Coandă MAV with various jet slot velocity as function of jet slot thickness / outer Radius R_o ; (a) $PM2$; (b) $PM3$.

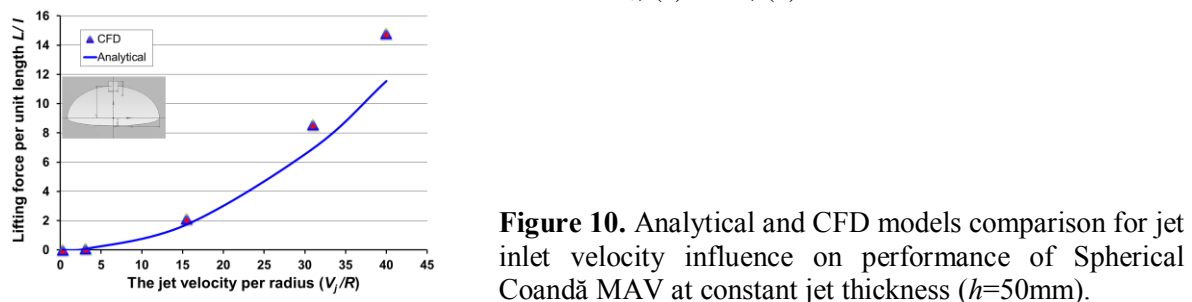


Figure 10. Analytical and CFD models comparison for jet inlet velocity influence on performance of Spherical Coandă MAV at constant jet thickness ($h=50\text{mm}$).

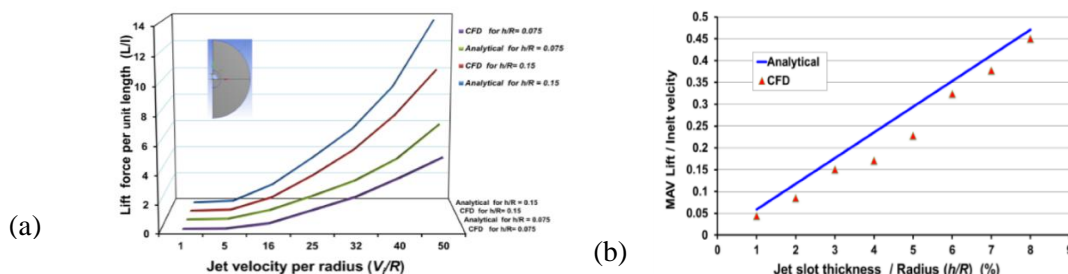


Figure 11. Performance measure comparison between mathematical and CFD models for Cylindrical Coandă MAV for various (a) Inlet velocity and (b) Jet slot thickness

Relatively good qualitative agreements between the theoretical results and CFD simulations shown there lend support to the present analysis, noting that in the analytical study many simplification have

been introduced, while in the CFD simulation, the full Navier-Stokes equation for incompressible fluid was used.

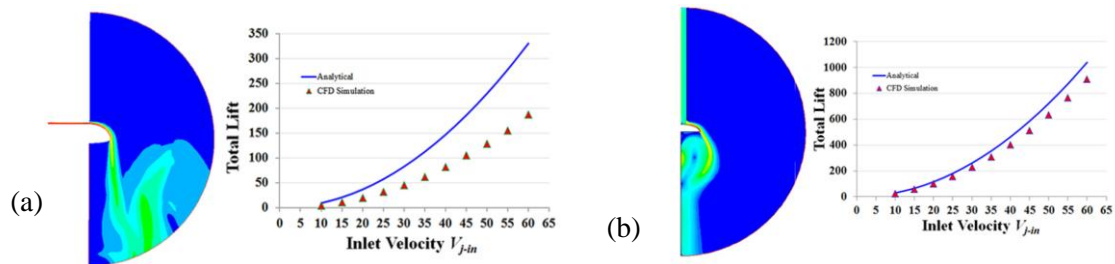


Figure 12. Lift versus input jet velocity for similar configuration considered in (a) Mirkov and Rasuo [16], (b) Ghozali [18]

The effect of viscosity that can be revealed by CFD simulation as exemplified by Figure12 for two different locations of the Coandă jet introduction. The CFD images exhibited in Figure12 (a) and (b) show the velocity magnitude contours for the given configuration and inlet conditions for cases considered by Mirkov and Rasuo [16-17] and Ghozali [18].

Meticulous attempts and grid sensitivity studies on the size of the mesh cells have been performed to enable plausible visualizations of the flow around the whole body with best details.

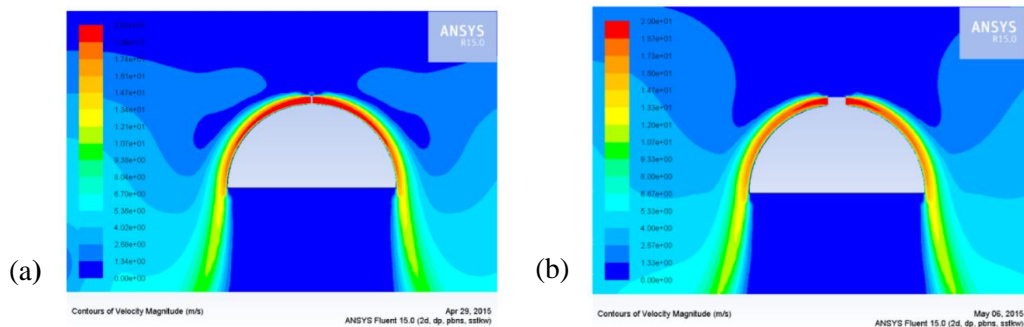


Figure13. Symmetrical Coandă effect - velocity magnitude contour with different inlet radial position; a) $Ri=5$ mm; b) $Ri=50$ mm

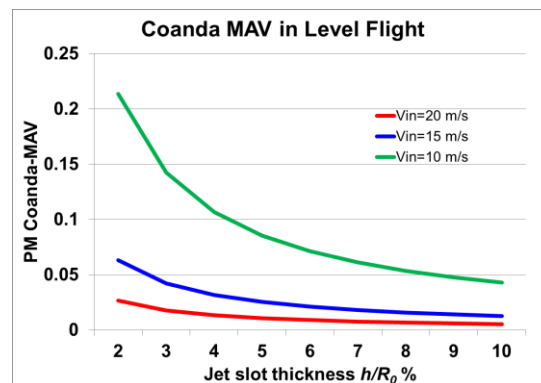


Figure 14. Coandă MAV Performance Measure as a function of jet slot thickness for various cruising velocity, calculated using Eq. (29) and CFD simulation for a baseline Coandă MAV configuration.

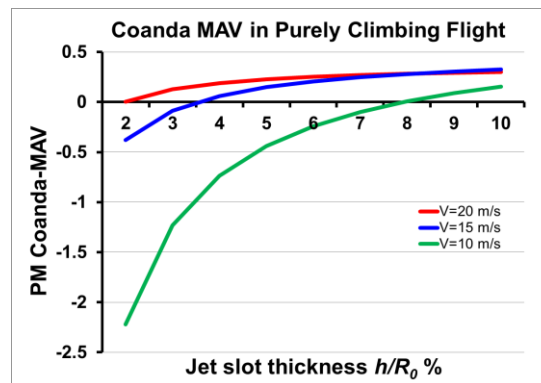


Figure15. Coandă MAV Performance Measure as a function of jet slot thickness for various climbing rate (velocity), calculated using Eq. (31) and CFD simulation for a baseline Coandă MAV configuration.

The numerical study was performed with a moderately small Reynolds number, $Re = 68458$, based on mean velocity and jet inlet height. The velocity across the inlet, which has a thickness of 0.05 m, is uniform ($V_{j-in} = 20$ m/s). The number of the mesh cells was 52830, and the mesh quality was found to be acceptable. The orthogonality quality was $4.96943e-01$, which is acceptable from the ANSYS orthogonality quality requirements. Results obtained on the influence of the inlet jet radius on the air vehicle performance (lift) investigated using CFD simulation for two inlet jet radius, $Ri = 5$ mm and $Ri = 50$ mm are presented as velocity magnitude contours shown in Figure13.

For translatory flight, some examples of Performance Measures simulation studies for Coandă MAV in purely level and climbing flights are exhibited by Figs. 14 and 15. The figures are obtained using equations (29) and (31) and CFD simulation for level and climbing flights, respectively.

6. Conclusions

A comprehensive effort has been made to analyze and describe the governing equations applicable to Coandă MAV in hover and translatory motion utilizing first principles as articulated in fluid dynamics and flight mechanic, using conservation principles for a control volume and free-body diagram for the application of Newton's law of motion. The paper establishes the basic working relationships among various relevant variables and parameters governing the aerodynamics forces and performance measures of Coandă MAV in hover and translatory motion. CFD simulations for a Coandă MAV generic model are carried out to gain insight into the flow situation, establishing the analytical model and validating it subject to the theoretical assumptions. The mathematical model and derived performance measures are shown to be capable in describing the physical phenomena of the flow field of the semi-spherical Coandă MAV. Comparison with CFD simulation serves also to assess the uncertainties and accuracy of the theoretical approach. In addition, the CFD computational and visualization studies, can provide further insight in revealing other characteristics of the flow field, and can assist further in-depth analysis, as well as in the design of experiments to that end. For example, to find out, under what conditions the effect of viscosity may cause the Coandă jet to separate. CFD visualization has certainly assisted the analytical work in assessing the application of fundamental conservation principle in continuum mechanics as well as elaborating the equation of motion for the flight dynamics of the Coandă MAV.

References

- [1] Gad-el-Hak M. *Flow Control - Passive, Active and Reactive Flow Management*. Cambridge University Press, London, United Kingdom, 448 pages 2000
- [2] Yi Liu, Lakshmi N. Sankar, Robert J. Englar, Krishan K. Ahuja. Numerical simulations of the steady and unsteady aerodynamic characteristics of a circulation control wing airfoil. *AIAA Paper*

2001-0704

- [3] Kweder J., Panther C.C., Smith J.E. Applications of circulation control, yesterday and today, *International Journal of Engineering, (IJE)* 195:, vol.4 (5), pp. 411-429, 2011.
- [4] Djojodihardjo H. and Thangarajah N. Research, development and recent patents on aerodynamic surface circulation control-A critical review. *Recent Patents on Mechanical Engineering* .vol. 7, pp. 1-37, 2014.
- [5] Djojodihardjo H. Progress and development of Coandă jet and vortex cell for aerodynamic surface circulation control—An overview. *The SIJ transactions on advances in space research & earth exploration (ASREE)*, Vol.1, No.1, September-October 2013
- [6] Rumsey CL, Nishino T. Numerical study comparing RANS and LES approaches on a circulation control airfoil. *International Journal of Heat and Fluid Flow* 32: 847-864, 2011.
- [7] Tongchitpakdee C., Benjanirat S., Sankar L.N. Numerical studies of the effects of active and passive circulation enhancement concepts on Wind Turbine Performance. *Journal of solar energy engineering transactions of the ASME*; 128: 432 – 444, 2006.
- [8] Hamid, MFAH, Djojodihardjo, H., Suzuki, S. and Mustapha, F. Numerical assessment of Coanda Effect as airfoil lift enhancer in wind-turbine configuration. *Regional conference on mechanical and aerospace technology* Bali, February 9 – 10, 2010
- [9] Djojodihardjo H., Abdul-Hamid M. F., Jaafar A. A., Basri S., Romli F. I., Mustapha F., Mohd-Rafie A. S. and Abdul-Majid D. L. A. Computational study on the aerodynamic performance of wind turbine airfoil fitted with Coandă Jet. *Journal of renewable energy*, volume 2013, Article ID 839319, 17 pages, 2013
- [10] Ahmed R.I., Djojodihardjo H., Abu Talib A.R., Abd Hamid M.F. Application of Coandă jet for generating lift for micro air vehicles – Preliminary design considerations, *Applied Mechanics and Materials* Vol. 629, pp. 139-144, 2014. URL: <http://www.scientific.net/AMM.629.139>
- [11] Ahmed R.I., Djojodihardjo H., Abu Talib A.R., Mohd-Rafie A. S., First Principle Analysis of Coandă Micro Air Vehicle Aerodynamic Forces for Preliminary Sizing" , *Aircraft Engineering and Aerospace Technology*, DOI: 10.1108/AEAT-03-2015-0080.R2 ,2015.
- [12] Djojodihardjo H. Ahmed R.I. An analysis on the lift generation for Coandă Micro Air Vehicles. *IEEE, ICARES conference proceeding*, Yogyakarta, Nov. 2014
- [13] Djojodihardjo, H., Ahmed, R.I., Thalib, A.R.A. and Rafie, M.A.S. Analytical and CFD visualization studies of Coandă MAV, *Proceedings*, The 13th Asian Symposium on Visualization, Novosibirsk, Russia, June 22–26, 2015,
- [14] Mamou, M. and Khalid, M. Steady and unsteady flow simulation of a combined jet flap and Coandă jet effects on a 2D airfoil aerodynamic performance. *Revue des Energies Renouvelables CER'07* Oujda 55 – 60, 2007
- [15] Schroyen, M. Van Tooren, M. MAV propulsion system using the Coandă effect. *45th AIAA/ASME /SAE/ASEE Joint Propulsion Conference & Exhibit* Denver, 2009.
- [16] Mirkov, N. and Rasuo, B. Numerical simulation of air jet attachment to convex walls and applications, *ICAS* 2010-621
- [17] Mirkov, N. and Rasuo, B. Maneuverability of a UAV with Coandă Effect based lift production, *ICAS* 2012-617
- [18] Ghozali, D. Analysis of Coandă Effect using computational-fluid-dynamic, Thesis, *Universitas Gajah Mada*, Indonesia, 2013.

Acknowledgments

The authors would like to thank Universiti Putra Malaysia (UPM) for granting Research University Grant Scheme (RUGS) No.9378200, and the ministry of higher education ERGS: 5527088 ; FRGS:5524250 under which the present research is carried out.